SOURCE PARAMETERS OF THE 2004 KOBARID (WESTERN SLOVENIA) SEISMIC SEQUENCE

G. Franceschina[1] and S. Gentili[2]

[1] Istituto Nazionale di Geofisica e Vulcanologia, Sezione di Milano-Pavia, Milano, Italy

[2] Istituto Nazionale di Oceanografia e di Geofisica Sperimentale, Centro Ricerche Sismologiche, Cussignacco, Udine, Italy

Introduction. The Kobarid area (western Slovenia) was struck by two seismic sequences in 1998 and 2004. Corresponding mainshocks, occurred on April 12, 1998 and July 12, 2004, had magnitude M_W=5.7 and M_W=5.2, respectively and were located 2.6 km away from each other. Both of them were recorded by the Friuli-Venezia Giulia Seismometric Network, managed by the Istituto Nazionale di Oceanografia e di Geofisica Sperimentale (OGS), installed in north-eastern Italy (http://www.crs.inogs.it). During the sequences, the network recorded hundreds of aftershocks and both standard locations and duration magnitude (M_D) estimations were performed. The seismic activity lasted 198 and 135 days, respectively and consisted of 700 events with M_D in the range [1.5, 4.6] and 300 events with M_D in the range [1.1, 3.6], respectively (Bressan *et al.*, 2009).

The two sequences occurred close to the Italian border, along the valley of the Lepenica river (Bragato *et al.*, 1998) in western Slovenia. The valley belongs to the NW-SE oriented Slovenian basin, in a region bounded between the Julian carbonate platform to the north and the Dinaric carbonate platform to the south (Bressan *et al.*, 2009). In particular, the seismicity was detected along the Ravne fault, a near vertical extended right-lateral strike slip fault zone trending NW-SE belonging to the Idrija fault system.

In this work, we estimate the seismic moment, M_0, the corner frequency, f_C, the Brune stress drop, $\Delta\sigma_B$, the apparent stress, σ_a and the radiated energy, E_S, of the mainshock and of 164 aftershocks of the Kobarid (2004) seismic sequence. The obtained results are compared with two previous analysis performed in the same region, concerning the source parameter scaling of the background seismicity (Franceschina *et al.*, 2006) and of other seismic sequences (Bressan *et al.*, 2007) occurred in the area. The Kobarid (1998) sequence has been investigated in the latter work.

Earthquakes are selected based on the duration magnitude reported in the Friuli-Venezia Giulia seismic bulletin (http://www.crs.inogs.it): all events with $M_D \geq 2.0$ are considered. For source parameters estimation, we employ the re-locations performed by tomography (Bressan *et al.*, 2009) and we uniformly re-compute the magnitudes in terms of local magnitude, M_L, using a specific attenuation relationship calibrated for the region (Bragato and Tento, 2005). Re-locations confirm that the seismic activity of the sequence affected an area of about 10 km radius around the mainshock epicenter (Gentili and Bressan, 2008) and that aftershocks were clustered between 4 and 6 km depth in an area weakly affected by the 1998 sequence. The focal plane solution of the mainshock evidences a dextral strike-slip motion concordant with the Ravne fault orientation and very similar to the focal mechanism of the mainshock of the 1998 sequence. On the contrary, the largest aftershocks are characterized by different types of focal mechanism and variable planes orientation probably related to the fault strength heterogeneities evidenced by the tomography of the area (Bressan *et al.*, 2009).

The stations of the Friuli-Venezia Giulia Seismometric Network recorded the sequence at distances ranging from 12 to 185 km. In order to improve the reliability of results, we select only stations located up to 100 Km epicentral distance from the Kobarid area and to account for possible local amplifications we also compute standard H/V spectral ratios (HVSR - Lermo and Chávez-García, 1993) for all the selected stations. This method assumes that the vertical component of the seismogram is not affected by the subsurface structure of the site and provides a rough estimate of site amplification (Field and Jacob, 1995).

For the source parameters estimation, we adopt a frequency domain analysis and compute the source spectrum from the SH pulses observed on velocity time series recorded at each selected station, after correction for geometrical spreading, scattering and anelastic attenuation. Generally, source spectra inferred from the data recorded by stations with negligible H/V amplifications, show a good fit with a ω^{-2} model. In this work, we adopt the Brune (1970; 1971) and the Boatwright

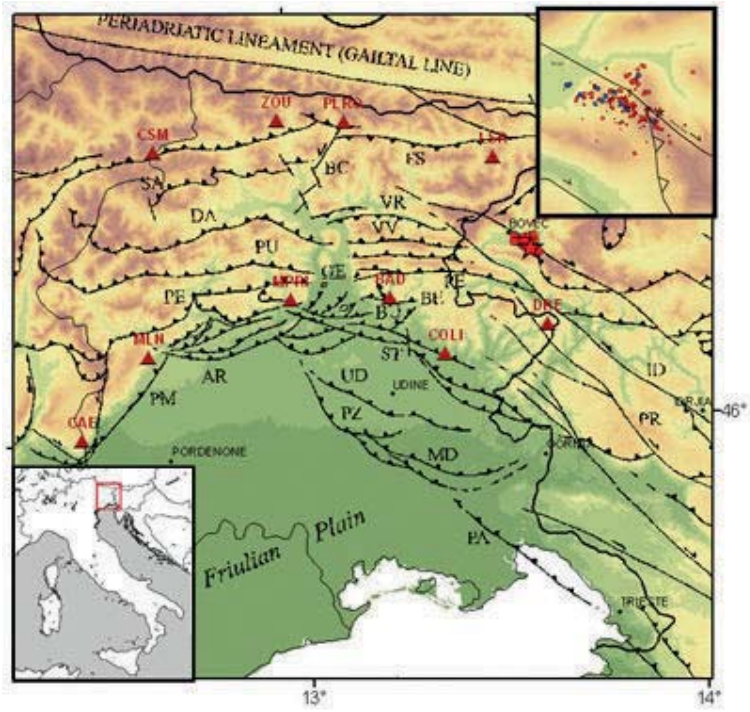

Fig. 1 - Location of the 2004 Kobarid sequence and main tectonic features of the region. In the main panel, the red star, red circles and red triangles indicate the mainshock epicenter, epicenters of the selected aftershocks and recording stations, respectively. Left-bottom inset shows the location of the analysed area. Right-top inset shows the epicentral area: blue symbols mark the epicenters of events with known focal mechanism.

(1980) models in order to infer single-station source parameters and we compute the earthquake source parameters as geometrical means of the corresponding distributions.

Data selection and processing. The analysed data are 3D velocity records obtained during the period from July 2004 to December 2004 by the Lennartz LE-3D seismometers of the Friuli-Venezia Giulia Seismometric Network. As previously mentioned, a careful data selection is performed in order to improve the results reliability. By selecting only events with $M_D \geq 2.0$ we obtain 1108 3D records from 14 seismic stations and the further selection, based on the station-to-receiver epicentral distance, R_E, performed by imposing $R_E < 100$ km, reduces to 10 the number of selected stations (see Fig. 1). The influence of possible site effects on the results has been investigated by computing the H/V spectral ratio for all these stations by adopting 8 s duration time windows. The result of this analysis, in accordance with previous works of Tento (2001) and Bragato and Slejko (2005), shows that there are three stations (PLRO, COLI and DRE) particularly relevant for site effects. These stations show spectral amplifications up to 3-4 over the whole frequency band adopted in our analyses. In source parameters computation, we do not consider the records obtained at PLRO, COLI and DRE.

A further selection of the records based on the signal to noise ratio, *S/N*, is performed in order to eliminate too noisy traces and to infer the useful frequency band $[f_a, f_b]$ for both local magnitude, M_L, computation and source parameters estimation. We impose $S/N \geq 3.0$ obtaining f_a in the range [0.2, 18] Hz and f_b in the range [18, 30] Hz, depending on the analysed signal. The selected 3D records are 869, corresponding to 166 events. For both the M_L and the source parameters computation we impose constraints on f_a and on the mean of the logarithm of *S/N* in the selected frequency band, $<Log(S/N)>$. Concerning M_L, we require $f_a \leq 1.0$ Hz and $<Log(S/N)> \geq 1.5$; for the source parameters we add the records characterized by $f_a > 1.0$ Hz but on condition that in the central part of the useful frequency band ([4, 16] Hz) the signal-to-noise ratio is sufficiently high. By adopting this criterion, we finally select traces with $1.1 \leq <Log(S/N)> \leq 6.1$. For computing M_L we simulate the response of a Wood-Anderson seismograph and calculate the magnitude on the

horizontal components of the ground motion, according to Hutton and Boore (1987) and Bragato and Tento (2005). The range of the obtained values is [0.8, 5.3], confirming that in this catalogue, M_D overestimates M_L for $M_L < 3.5$ (Gentili *et al*., 2011).

The ground velocity spectrum is calculated after correcting the recorded time series for the baseline and for the instrument response. A no-causal eight poles Butterworth filter is also applied between the above inferred frequencies f_a and f_b in order to reduce the influence of noise on the data selected for the analysis. Variable-length windows with durations ranging from 1.0 to 10.9 s are manually picked starting from the first onset of the direct S waves using the transverse component of the ground velocity. Afterwards, the amplitude Fourier spectrum of SH waves is computed by applying a 2% cosine taper and padding with zeros before applying the FFT algorithm. Finally, the resulting spectrum is smoothed through the function introduced by Konno and Ohmachi (1998) using $b = 20$. The final data set is composed of 492 3D records corresponding to 165 earthquakes recorded by 7 stations of the network and characterized by hypocentral distances ranging from 18 to 96 km (see Fig. 1). The location of the selected earthquakes, obtained through tomography re-location by Bressan *et al.,* (2009) is characterized by high accuracy, with horizontal and vertical location errors not exceeding 0.05 and 0.1 km, respectively (Bressan *et al.,* 2009).

Source parameter estimation. The SH-waves displacement amplitude Fourier spectrum observed at hypocentral distance R and modeled by $D(R, f) = D_S(f) \cdot A(R, f)$, is corrected for the attenuation term $A(R, f)$, given by:

$$A(R, f) = (1 / R) \cdot exp (- \pi f k (S, R_E)) \cdot exp (- \pi f R / (\beta , Q_d (f))) \quad (1)$$

where R_E is the epicentral distance and , is the S waves velocity. The frequency dependent part of the quality factor is modeled as $Q_d(f) = 251 \cdot f^{0.7}$ according to Bianco *et al.* (2005) and the spectral decay parameter k (Anderson and Hough, 1984) is obtained for each station considering the results of a previous work dealing with the high frequency attenuation of the area (Gentili and Franceschina, 2011). After that, Brune (1970) and Boatwright (1980) models are employed to estimate seismic moment, M_0, corner frequency, f_C and radiated energy, E_S, from the best fit source spectrum, $D_S(f)$. In detail, starting from the signal windowed on the SH pulse, we calculated $V_{obs}(f)$ and $D_{obs}(f)$, the observed amplitude velocity and displacement spectra corrected for attenuation by the term $A(R, f)$. Afterwards, we calculate the corner frequency, f_C , according to Andrews (1986):

$$f_c = \frac{1}{2\pi} \sqrt{\frac{\int_{f_a}^{f_b} V_{obs}^2(f) df}{\int_{f_a}^{f_b} D_{obs}^2(f) df}} \quad (2)$$

the seismic moment, M_0 , as in Franceschina *et al.* (2006):

$$Log_{10}(M_0) = \frac{1}{f_b - f_a} \int_{f_a}^{f_b} \left\{ Log_{10}\left[D_{obs}(f) \right] - Log_{10} \frac{\frac{F_S R_{\theta\phi}}{4\pi\rho\beta^3}}{1 + \left(\frac{f}{f_c} \right)^2} \right\} df \quad (3)$$

and the radiated seismic energy, E_S, according to the spectral theory of Boatwright (1980):

$$E_S = \frac{2\rho\beta}{e_\beta (F_S R_{\theta\varphi})^2} \int_{f_a}^{f_b} V_{obs}^2(f) df \quad (4)$$

$R_{\theta\varphi}$ is an average radiation pattern and we assumed $R_{\theta\varphi} = 0.38$ according to most of the events of the analysed dataset having known focal mechanism; F_S is the free surface effect ($F_S = 2$); β is

the density (assumed equal to 2.7 g/cm^3); , is the S waves velocity (assumed equal to 3.3 km/s); f_a and f_b define the frequency band useful for the analysis, established through the signal-to-noise ratio estimation as above described. In Eq. (4), we assume the dimensionless fractional energy flux for shear waves $e_{\beta,} = 1/2\pi$ (Boatwright, 1980) and correct for the effect of bandwidth limitation according to Ide and Beroza (2001).

For each earthquake, geometric means $<M_0>$, $<f_C>$ and $<E_S>$ are computed from single station estimates $M_0(i)$, $f_C(i)$ and $E_S(i)$, respectively according to:

$$\begin{aligned} &Log <M_0> = \sum_i Log\, M_0(i) / N \\ &Log <f_C> = \sum_i Log\, f_C(i) / N \\ &Log <E_S> = \sum_i Log\, E_S(i) / N \end{aligned} \quad (5)$$

where N is the number of stations that recorded the event.

Brune radius, r_B, Brune stress drop, $\Delta\sigma_B$, and apparent stress, σ_a, are calculated by:

$$\begin{aligned} &<r_B> = 2.34\, \beta / (2\pi <f_C>) \\ &<\Delta\sigma_B> = <M_0> <f_C>^3 / (49\, \beta)^3 \\ &<\sigma_a> = \rho\beta^2 <E_S> / <M_0> \end{aligned} \quad (6)$$

Misfits between observed and model spectra calculated with the single-station and with the average estimates of source parameters are computed as:

$$m_s = \int_{fa}^{fb} (Log\ D_S\ (f, M_0(i), f_c(i)) - Log\ D_{obs}(f))\, df \quad (7)$$

and

$$m_E = \int_{fa}^{fb} (Log\ D_S\ (f, <M_0>, <f_c>) - Log\ D_{obs}(f))\, df \quad (8)$$

respectively.

Considering that the region interested by the sequence is limited in space and that the locations of the earthquakes are accurate, we also applied the Empirical Green Function (EGF) technique with the aim to validate the results obtained with the above method. In the EGF technique, small earthquakes located in close proximity to a larger one, and with the same focal mechanism, are used as empirical Green functions in order to remove both propagation and site effects from the records of the larger earthquake. We apply the EGF method to a subset of the selected data (Abercrombie and Rice, 2005) by selecting couples of events with $\Delta R < 500$ m and $\Delta M_L > 1.0$. We obtain 7 master events with $2.7 \le M_L \le 5.3$ corresponding to 30 event pairs and 78 record pairs from 9 stations and 14 secondary events with $1.2 \le M_L \le 2.4$. For each pair we estimate the spectral ratio $\Omega(f)$ and we model it as:

$$\Omega(f) = (M_0^{(1)} / M_0^{(2)}) \cdot [1 + (f / f_C^{(2)})^2] / [1 + (f / f_C^{(1)})^2] \quad (9)$$

where $f_C^{(1)}$ and $f_C^{(2)}$ are the corner frequencies of the strongest and of the smaller event, respectively while $M_0^{(1)}$ and $M_0^{(2)}$ are their corresponding seismic moments. A three parameters minimization procedure allows to estimate $f_C^{(1)}$, $f_C^{(2)}$ and the ratio $M_0^{(1)}/M_0^{(2)}$ and the final value of $f_C(i)$ of the i^{th} event is estimated as geometrical mean of the values obtained with all the pairs containing that event.

Results. The results inferred by applying Eqs. (2)-(6) to the obtained SH-wave spectra are summarized in Table 1, that lists the source parameters of the mainshock and of the strongest ($M_L \ge 3.0$) aftershocks of the sequence, together with the ranges of variability of the aftershocks parameters. Generally, SH-wave spectra corrected for attenuation, show a good fit with the Brune model, with misfit values such that $|m_E| < 0.55$. For the mainshock, we obtain M_0=3.5x10^{16} Nm, f_C =0.8 Hz and E_S = 2.4x10^{12} J, with multiplicative standard errors, *MSE*, of 1.2, 1.2 and 1.3, respectively. Seismic moments, corner frequencies and radiated energies of the selected aftershocks

Tab. 1 - Source parameters of the mainshock (Code=0392) and of the strongest ($M_L \geq 3.0$) aftershocks of the Kobarid (2004) seismic sequence and range of variability of the aftershocks parameters (last row). In the last row, the multiplicative standard errors (MSE) represent the average errors obtained on aftershocks parameters. Corner frequencies (and corresponding MSE) inferred by the EGF method are also reported for comparison.

Code	Date [YYMMDD]	Time [hh:mm:ss]	Lon [°E]	Lat [°N]	H [Km]	M_L	M_0 [Nm]	f_c [Hz]	r_B [m]	a [MPa]	E_s [J]	s [MPa]	M_o *MSE*	f_c *MSE*	a *MSE*	E_s *MSE*	a *MSE*	$f_c^{(EGF)}$ [Hz]	$f_c^{(EGF)}$ [*MSE*]
0392	040712	13-04.07	13.610	46.310	6.0	5.3	3.5E+16	0.8	1465	4.89	2.4E+12	1.94	1.2	1.2	1.8	1.3	1.4	0.8	1.3
0471	040712	16-26.59	13.620	46.323	6.7	3.1	1.1E+14	2.3	525	0.33	4.5E+08	0.12	1.4	1.2	2.1	1.6	1.8	-	-
0907	040714	04-37.38	13.602	46.319	4.9	3.5	1.8E+14	2.1	566	0.44	6.6E+08	0.10	1.4	1.3	2.2	1.6	1.8	1.9	-
1178	040717	19-18.40	13.612	46.327	4.6	3.0	7.8E+13	2.5	468	0.33	2.8E+08	0.10	1.3	1.2	2.0	1.8	1.7	-	-
1306	040721	09-50.21	13.589	46.322	5.0	3.0	5.9E+13	3.2	374	0.49	3.0E+08	0.15	1.4	1.2	2.1	1.7	1.2	3.6	1.7
1362	040723	13-52.08	13.576	46.319	4.8	3.1	4.0E+13	3.2	371	0.35	2.1E+08	0.15	1.3	1.1	1.6	1.6	1.7	-	-
1793	040818	14-24.24	13.595	46.318	4.9	3.2	4.3E+13	4.2	230	1.55	7.2E+08	0.48	1.4	1.2	2.0	2.4	2.5	4.8	1.4
2317	041106	17-09.20	13.623	46.303	6.3	3.1	5.8E+13	4.1	288	1.07	7.4E+08	0.36	1.3	1.2	1.7	1.7	1.8	-	-
after shocks	040712 - 041208		13.564 13.662	46.285 46.332	2.5 10.1	0.8 3.5	3.3E+11 1.8E+14	1.9 12.4	95 638	0.03 1.55	2.0E+05 7.4E+08	0.01 0.48	1.3	1.2	2.0	1.5	1.9	-	-

are in the ranges [$3.3x10^{11}$, $1.8x10^{14}$] Nm, [1.9, 12.4] Hz and [$2.0x10^{5}$, $7.4x10^{8}$] J, respectively. The adopted procedure allows us to reduce errors on both mainshock and aftershocks source parameters. Indeed, parameters which are directly estimated from the spectrum have *MSE* values not exceeding 2.5. On average these parameters are characterized by $MSE(M_0)$=1.3, $MSE(f_C)$=1.2 and $MSE(E_S)$=1.5.

The seismic moment of the mainshock is in good agreement with the value of $2.6x10^{16}$ Nm estimated by Bressan *et al.* (2007) with a method similar to the one described in this paper and it is slightly lower than the Harvard CMT catalogue solution of $7.1x10^{16}$ Nm.

The EGF method applied to the 7 master events selected for this analysis confirms the values of f_C obtained with the spectral method. In particular, the strongest aftershocks have corner frequencies in the range [2.1, 5.2] Hz (see Tab. 1). Instead, according to Abercrombie *et al.* (2012), this technique often results in an underestimation of the corner frequency when applied to secondary

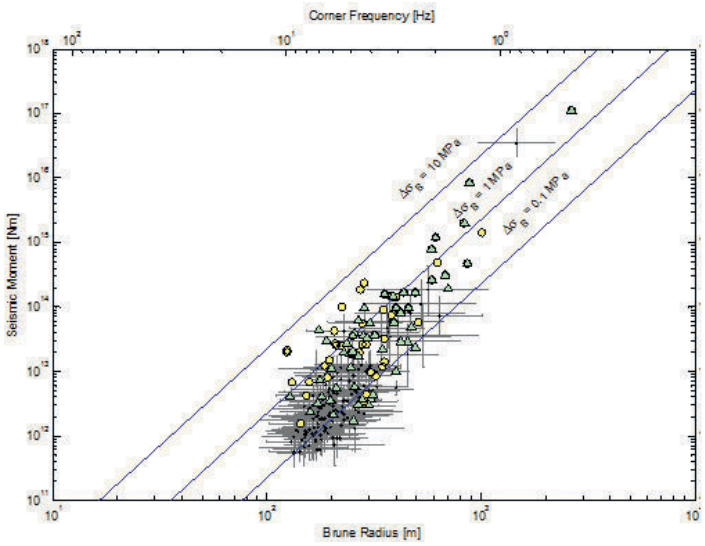

Fig. 2 - Seismic moment as function of Brune radius and corner frequency. Black dots: results of this work (corresponding multiplicative errors are also shown); yellow circles: Franceschina *et al.* (2006) data; green triangles: Bressan *et al.* (2007) data. Blue lines: constant values of Brune stress drop.

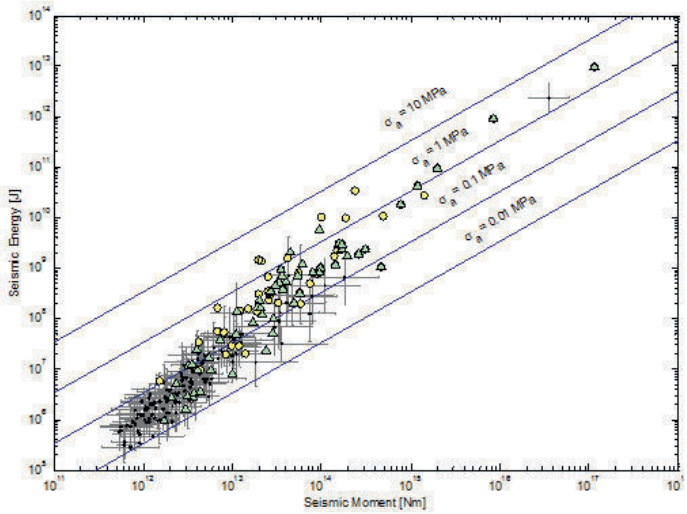

Fig. 3 - Radiated seismic enargy as a function of seismic moment. Black dots: results of this work (corresponding multiplicative errors are also shown); yellow circles: Franceschina *et al*. (2006) data; green triangles: Bressan *et al*. (2007) data. Blue lines: constant values of apparent stress.

events.

The scaling of source dimension with respect to seismic moment is shown in Fig. 2, where the results obtained in this work are compared with the estimates of source parameters concerning the background seismicity of the region (Franceschina *et al.*, 2006) and other seismic sequences recorded in the same area (Bressan *et al.*, 2007). The present results are consistent with the previous scaling and show an increase of the Brune radius with M_0 for seismic moments ranging between 3.0×10^{11} and 1.0×10^{17} Nm. The linear fit of the seismic moment estimates versus corner frequencies gives: $Log\ M_0 = -4.64\ Log\ f_C + 15.9$ and evidences non-self-similarity properties of the analysed events.

Radiated energies also scale with moments showing that for this sequence, the stress release, in terms of apparent stress, increases with M_0. In Fig. 3, we compare the present estimates of E_S with results of the above mentioned papers. Radiated energies increase with seismic moments and E_S values appear well correlated with M_0 by the empirical relationship: $Log\ E_S = 1.53\ Log\ M_0 - 12.5$. The data show a lower dispersion with respect to those of Fig. 2 thus evidencing a clear increase of apparent stress with M_0.

The stress release of the 165 events of the Kobarid (2004) sequence selected in this analyses thus shows non-self-similarity properties evidenced by the increase of the Brune stress drop and of the apparent stress with seismic moment (see the blue lines in Fig. 2 and Fig. 3, corresponding to different constant values of $\Delta\sigma_B$ and σ_a, respectively). According to Mori *et al.* (2003), the trends of both $\Delta\sigma_B$ and σ_a with moment can be explained by considering that large earthquakes tend to be more complex then small events and characterized by a greater high-frequency content, therefore radiating more energy for unit slip and unit fault area.

Acknowledgements. We would like to thank Gianni Bressan for his valuable discussions and suggestions. The management of the Seismometric Network of Friuli-Venezia Giulia is financially supported by the Civil Protection of the Regione Autonoma Friuli-Venezia Giulia. The Seismometric Network of Veneto is owned by the Regione Veneto. We are grateful to all the OGS staff of the Dipartimento Centro Ricerche Sismologiche at Udine for managing the two networks. This research has benefited from funding provided by the by the Civil Protection of the Regione Autonoma Friuli-Venezia Giulia and by "Stogit S.p.A. – Eni".

References

Abercrombie R.E. and Rice J.R.; 2005: Can observations of earthquake scaling constrain slip weakening? Geophys. J. Int., 162, 406-424, doi: 10.1111/j.1365-246X.2005.02579.x.

Abercrombie R.E., Walter W. and Gök R.; 2012: Comparison of Direct and Coda Wave stress drop measurements for the Wells, Nevada, earthquake sequence, (in prep).

Anderson J.G. and Hough S.; 1984: A model for the shape of Fourier amplitude spectrum of acceleration at high frequencies. Bull. Seism. Soc. Am., 74, 1969-1994.

Andrews D.J.; 1986: Objective determination of source parameters and similarity of earthquakes of different size. In: Das S., Boatwright J., Sholz C.H. (eds), Earthquake Source Mechanics, American Geophysical Union, Geophysical monograph, 37, pp. 259-267.

Bianco F., Del Pezzo E., Malagnini L., Di Luccio F. and Akinci A.; 2005: Separation of depth-dependent intrinsic and scattering seismic attenuation in the northeastern sector of the Italian Peninsula. Geophys. J. Int., 161, 130-142.

Boatwright J.; 1980: A spectral theory for circular seismic sources: simple estimates of source dimension, dynamic stress drop and radiated energy. Bull. Seism. Soc. Am., 70, 1–27.

Bragato P.L., Bernardis G., Bressan G., Candido M., Durì G., Govoni A., Ponton F., Slejko D., Snidarcig A. and Urban S.; 1998: Il terremoto di Bovec (Alpi Giulie) del 12 aprile 1998: analisi dei dati sismometrici. GNGT, Atti del 17° Convegno Nazionale, Roma, 10-12 Novembre 1998, 09.06.

Bragato P.L. and Slejko D.; 2005: Empirical Ground-Motion Attenuation Relations for the Eastern Alps in the Magnitude Range 2.5-6.3. Bull. Seism. Soc. Am., 95, 252-276.

Bragato P.L. and Tento A.; 2005: Local Magnitude in Northeastern Italy. Bull. Seism. Soc. Am., 95, 579–591.

Bressan G., Gentile G.F., Perniola B. and Urban S.; 2009: The 1998 and 2002 Bovec-Krn (Slovenia) seismic sequences: aftershock pattern, focal mechanisms and static stress changes. Geophys. J. Int., 179, 231–253.

Bressan G., Kravanja S. and Franceschina G.; 2007: Source parameters and stress release of seismic sequences occurred in the Friuli-Venezia Giulia region (Northeastern Italy) and in Western Slovenia. Phys. Earth Planet. In. 160, 192-214.

Brune J.N.; 1970: Tectonic stress and the spectra of seismic shear waves from earthquakes. J. Geophys. Res., 75, 4997–5009.

Brune J.N.; 1971: Correction. J. Geophys. Res., 76, 5002.

Field, E.H. and Jacob K.H.; 1995: A comparison and test of various site-response estimation techniques, including three that are not reference-site dependent. Bull. Seism. Soc. Am., 85, 1127-1143.

Franceschina G., Kravanja S. and Bressan G.; 2006: Source parameters and scaling relationships in the Friuli-Venezia Giulia (Northeastern Italy) region. Phys. Earth Planet. In., 154, 148-167.

Gentili S. and Bressan G.; 2008: The partitioning of radiated energy and the largest aftershock of seismic sequences occurred in the northeastern Italy and western Slovenia. J. Seismology, 12, 343–354.

Gentili S. and Franceschina G.; 2011: High frequency attenuation of shear-waves in Southeastern Alps and Northern Dinarides. Geophys. J. Int., 185, 1393–1416.

Gentili S., Sugan M., Peruzza L. and Schorlemmer D.; 2011: Probabilistic completeness assessment of the past 30 years of seismic monitoring in northeastern Italy. Phys. Earth Planet. In., 186, 81 – 96.

Hutton L.K. and Boore D.M.; 1987: The ML scale in southern California. Bull. Seism. Soc. Am., 77, 2074–2094.

Ide S. and Beroza G.C.; 2001: Does apparent stress vary with earthquake size ?, Geophys. Res. Lett., 28, 3349-3352.

Konno K. and Ohmachi T.; 1998: Ground-Motion Characteristics Estimated from Spectral Ratio between Horizontal and Vertical Components of Microtremor. Bull. Seism. Soc. Am., 88, 228-241.

Lermo J. and Chávez-García F.C.; 1993: Site effect evaluation using spectral ratios with only one station. Bull. Seism. Soc. Am., 83, 1574–1594.

Mori J., Abercrombie R.E. and Kanamori H.; 2003: Stress drops and radiated energies of aftershocks of the 1994 Northridge, California, earthquakes. J. Geophys. Res. 108 (B11), 2545, doi:10.1029/2001JB00474.

Tento A.; 2001: La magnitudo locale del Friuli. Rapporto Tecnico IDPA (CNR), Milano, 23 pp.

THE 2010-2012 WESTERN-POLLINO SEISMIC SEQUENCE IN THE FRAMEWORK OF THE QUATERNARY SEDIMENTARY AND TECTONIC EVOLUTION OF THE MERCURE BASIN

P. Galli[1,2], B. Giaccio[2], M. Mancini[2], P. Messina[2], E. Peronace[2], G. Cavinato[2], A. Giocoli[3] and S. Piscitelli[3]

1 Dipartimento della Protezione Civile Nazionale, Roma

2 CNR-IGAG, Roma

3 CNR-IMAA, Potenza

Since June 2010, the Mount Pollino area has been affected by a continuous seismic swarm, made up by thousands low magnitude events (Mw<4.5; ISIDe, 2012), which are mainly grouped into two main clusters: one at the southwestern edge of the Pollino carbonate massif and the other at its western edge. The western cluster (Mormanno-Rotonda area; Mw max 3.7) partially matches the area of the Mercure Basin, an intermountain tectonic depression bounded northward by the ~N120 Castelluccio-Viggianello normal fault (CVF). Its infilling includes up to 350 m of continental Quaternary fluvial-lacustrine deposits (Gemina, 1963) which are at present dissected by the Mercure river, thus making accessible and investigable at least the upper part of the sedimentary sequence.

The focal mechanisms of the mainshocks (Fig. 1) and the hypocentral distribution of the seismic